Exactly solvable model for nonlinear light-matter interaction in an arbitrary time-dependent field

J. M. Brown,[1] A. Lotti,[2,3] A. Teleki,[4] and M. Kolesik[1,4]
[1]*College of Optical Sciences, University of Arizona, Tucson, Arizona 85721, USA*
[2]*Dipartimento di Scienza e Alta Tecnologia, Universitá dell' Insubria, I-22100 Como, Italy*
[3]*Centre de Physique Théorique, École Polytechnique, CNRS, F-91128 Palaiseau, France*
[4]*Department of Physics, Constantine the Philosopher University, Nitra, Slovakia*
(Received 4 December 2011; published 29 December 2011)

Exact analytic expressions are derived for the dipole moment and nonlinear current of a one-dimensional quantum particle subject to a short-range attractive potential and an arbitrary time-dependent electric field. An efficient algorithm for the current evaluation is described and a robust implementation suitable for numerical simulations is demonstrated.

DOI: 10.1103/PhysRevA.84.063424 PACS number(s): 32.80.Rm, 42.50.Hz, 42.65.Ky

I. INTRODUCTION

The original motivation for this work came from developments in the general area of optical filamentation in high-power femtosecond pulses. The models which underlie the theory and simulation of light-matter interactions at femtosecond time scales [1] evolved from approaches that worked well for longer time scales, and are based on a great deal of phenomenological description. In particular, what can be termed as the standard model in optical filamentation is actually a collection of independent components which parametrize Kerr nonlinearity, ionization in strong fields, ionization losses in the optical field, defocusing by free electrons, and possibly higher-order nonlinear effects [2]. In reality, these processes are intimately connected, and recent debates have made it evident that light-matter interactions at very short time scales require renewed attention. For example, observations of strong third-harmonic generation increasing in preformed plasmas [3] strongly suggest that plasma can contribute significantly to the nonlinear response. However, an alternative explanation was also proposed [4]. Another example is the discussion and controversy following experiments on higher-order Kerr-type nonlinearity [5] in femtosecond filaments. The fact alone that the basic filamentation physics could be questioned after years of research speaks to the weak foundations of the underlying theoretical models. What is needed is a self-consistent, first-principles-based approach, but the practical realization of such a program remains very difficult. That is why learning from exactly solvable models is a promising way to improve the current state of the art in the area; this paper aims to provide a useful tool for such investigations.

We study arguably the simplest possible system to describe light-matter interaction in which continuum-energy states play a crucial role. It is the well-known one-dimensional "atom" with a δ potential exposed to a time-dependent external field.

There are two sides to the results we present. First, we calculate exact formulas for the evolution of the current and/or dipole moment in an arbitrary time-dependent field. Despite the fact that the system has been studied for a long time in many different contexts, our results will greatly extend the utility of the model as a testbed system. Second, we have developed an efficient implementation for the induced current formulas. To help an interested reader in their practical application, we devote significant room to the numerical algorithm.

We envision two main areas in which our results will find practical application. In the simulation of femtosecond filaments, they will allow qualitative-level studies in which the weakest links in the standard model will be replaced by a self-consistent quantum model. For high-harmonic generation (HHG) modeling, we present an exactly solvable alternative to the strong-field approximation. Both the strong-field approximation and the model in this paper have only a single bound state plus a continuum of free states, therefore the range of physics that they capture is similar. The advantage of the present approach is that it is an exact solution valid throughout the full frequency bandwidth, including the fundamental as well as the highest harmonic frequencies.

II. MODEL

The quantum model we study in this paper describes a single particle subjected to a homogeneous external field and a short-range contact potential. The time-dependent Schrödinger equation for this "one-dimensional atom" can be written as

$$\left[i\partial_t + \tfrac{1}{2}\partial_x^2 + B\delta(x) - xF(t)\right]\psi(x,t) = 0. \tag{1}$$

Here, B is the strength of the Dirac δ interaction, and $F(t)$ stands for the intensity of a time-dependent electric field. Atomic units have been chosen to simplify the notation.

The above equation is merely symbolic unless a proper meaning is given to the δ potential. The precise Hamiltonian definition (see, e.g., [6,7]) of this system specifies the contact interaction as a condition which all functions that belong to the Hamiltonian domain must fulfill, namely,

$$2B\psi(0) = \frac{d\psi(0^-)}{dx} - \frac{d\psi(0^+)}{dx}, \tag{2}$$

which means that wave functions are continuous but exhibit a discontinuity in their derivative. For positive B, this gives rise to a single bound (ground) state,

$$\psi_G(x) = \sqrt{B}e^{-B|x|}. \tag{3}$$

Explicit expressions are known for all continuum (positive-energy) states, as well as for the Hamiltonian resolvent in the static field (see, e.g., [8,9]).

This toy model has often been utilized as a testbed in the area of strong light-matter interaction. As one would expect for an exactly solvable system, it has been studied for its mathematical properties and physical applications alike. For the mathematical aspects, we refer the reader to books on Schrödinger operators [10] and singular perturbations in differential operators [11]. For its physical implications, Geltman [12] investigated time-dependent ionization in strong electrostatic fields. Explicit results for the time dependence of the survival probability of the decaying ground state were given by Arrighini and Gavarini in [13], and also by Elberfeld and Kleber [14], who used this system to model tunneling from a quantum well and derived useful analytic results for an arbitrary time-dependent external field. Cavalcanti *et al.* [9] described generalizations to higher dimensions and made a connection between deviations from the exponential decay and long-lived resonances. Two short-range attractive potentials were used to describe molecular ionization in a static field [15], and a double δ potential was also studied by Álvarez and Sundaram [16]. A generalization to an arbitrary finite number of δ-potential interactions was given by Uncu *et al.* [17] as a model for impurities in GaAs/GaAlAs junctions. Villalba and González-Díaz introduced a δ potential into the Dirac equation [18]. Recently, we took advantage of the exact solvability of this system to gain insight into the possible manifestation of higher-order nonlinearity in strong optical fields [19].

There are numerous works in previously published literature which either investigate one-dimensional atom models themselves, or use them as tools to test and study numerical techniques and theories. Much of this work was done in the context of stabilization in strong fields [20]. Numerical and eigenstate expansions have been applied [21], and the Floquet method was also used [22] with the system discussed here. Approximate ionization rates were calculated in [23], and numerical simulations of photoionization were performed in [24]. More recently, there have been a number of papers in which various approximate and numerical methods are applied to one-dimensional systems, such as state-specific expansion [25], Kramers-Henneberger frame transformation [26], and least-squares fitting of time evolution [27]. This model also served as a testbed for numerical simulation techniques [28] and analytic theories [29,30].

Collectively, the works referenced above illustrate an interesting point, which perhaps remains valid in a wider context. Although the model including a short-range δ potential is formally exactly solvable, it is still far from trivial to extract useful information from it. Therefore, approximate approaches are often utilized, which unfortunately goes against the spirit of studying a model system in an exact setting. It is this fact that provides the motivation for this paper. Although this concrete system has been studied for a long time, exact solutions for arbitrary time-dependent external fields have not been published. We present such solutions together with a method to implement them in software.

The next section is devoted to the derivation of the probability current evolution for an arbitrary time-dependent field. The main result is stated for the current observable, while analogous expressions for the time-dependent dipole moment are summarized in the Appendix. In our final results, we exactly eliminate the component that is linear in the driving field $F(t)$. The rationale for doing so is that this model will be used to describe the nonlinear response, while linear medium properties can be efficiently incorporated using standard approaches. Next we discuss how to efficiently implement the nonlinear current formulas. Since this work mainly aims to present results concerning the δ-function atom model, we devote relatively small room to illustrations. These will verify that the results based on the analytic solution coincide with the direct numerical solution of the time-dependent Schrödinger equation (which requires orders of magnitude of more numerical effort), and that the implementation is robust, stable, and works accurately even in extreme regimes, such as for high-harmonic generation with long-wavelength driving pulses. In the last section, we briefly discuss various options that our results open for applications in the computer simulation of light-matter interactions.

III. INDUCED CURRENT: AN EXACT SOLUTION

One of the main difficulties when integrating the time-dependent Schrödinger equation and Maxwell equations is that the history of a quantum system must be calculated at each spatial point resolved by the Maxwell solver. This is necessary to extract time-dependent observables, and it requires resolution of the wave function in space. Our goal is to eliminate the spatial dimension from the quantum system, and derive expressions directly for the dipole moment and current observables. Elberfeld *et al.* [14] achieved this for the probability that the system remains in the ground state. We follow the same strategy and extend it for current and dipole calculations.

The solution for the wave function $\psi(x,t)$ can be cast in the form [14]

$$\begin{aligned}
\psi(x,t) &= \psi_F(x,t) + \psi_S(x,t),\\
\psi_F(x,t) &= \int dx'\, K_F(x,t|x',0)\psi_G(x'),\\
\psi_S(x,t) &= iB\int_0^t dt'\, K_F(x,t|0,t')\psi(0,t'),\\
\psi_G(x) &= B^{1/2}e^{-B|x|}.
\end{aligned} \tag{4}$$

The first term $\psi_F(x,t)$ represents the wave-packet evolution under the influence of the external field $F(t)$, but without the short-range potential. The second term $\psi_S(x,t)$ describes scattering from the δ potential followed by propagation in the field $F(t)$. In these equations, K_F is the Volkov propagator and ψ_G is the ground state (3). The Volkov propagator can be conveniently expressed through quantities related to the motion of a classical electron driven by $F(t)$, namely, classical position $x_{cl}(t)$, momentum $p_{cl}(t)$, and action $S_{cl}(t)$. Explicitly,

$$\begin{aligned}
K_F(x,t|x',t') &= e^{i\phi(x,t,x',t')}K_0(x-x_{cl}(t),t|x'-x_{cl}(t'),t'),\\
K_0(x,t|x',t') &= \frac{1}{\sqrt{2\pi i(t-t')}}e^{-\frac{(x-x')^2}{2i(t-t')}},\\
\phi(x,t,x',t') &= xp_{cl}(t) - x'p_{cl}(t') - [S_{cl}(t) - S_{cl}(t')],
\end{aligned} \tag{5}$$

and the classical quantities are obtained from $F(t)$ as

$$\begin{aligned} p_{cl}(t) &= -\int_0^t F(\tau)d\tau, \\ x_{cl}(t) &= \int_0^t p_{cl}(\tau)d\tau, \\ S_{cl}(t) &= \frac{1}{2}\int_0^t p_{cl}^2(\tau)d\tau. \end{aligned} \tag{6}$$

Before beginning the derivation, we would like to point out an important issue regarding practical implementation. It is obvious that for an initial condition given by the ground state, ψ_F and ψ_S do not have characteristics representative of the full solution. This means that significant cancellations occur between the two, which is dangerous numerically. It is therefore imperative to identify these cancellations and eliminate them before the numerical evaluation.

The observable of interest, which gives rise to current density in Maxwell's equations, is the total current contribution from one atom,

$$J(t) = \int_{-\infty}^{+\infty} J(x,t)dx, \tag{7}$$

where the probability current density

$$J(x,t) = \mathrm{Im}\{\psi^*(x,t)\nabla\psi(x,t)\} \tag{8}$$

can be given as a sum of the contributions originating in the two components of the wave function,

$$J(x,t) = \mathrm{Im}\{\psi_F^*\nabla\psi_F + \psi_F^*\nabla\psi_S + \psi_S^*\nabla\psi_F + \psi_S^*\nabla\psi_S\}. \tag{9}$$

A. Integral equation for $\psi(0,t)$

The full current (9) will be evaluated with the wave function expressed as in Eq. (4), which in turn requires knowledge of $\psi(x=0,t)$. This satisfies an integral equation obtained directly from (4),

$$\begin{aligned} \psi(0,t) = &\int_{-\infty}^{+\infty} dy K_F(0,t|y,0)\psi_G(y,0) \\ &+ iB\int_0^t dt' K_F(0,t|0,t')\psi(0,t'). \end{aligned} \tag{10}$$

It is convenient to use the following ansatz to eliminate, at least partially, rapid phase changes:

$$\psi(0,t) = \sqrt{B}A(t)e^{-iS_{cl}(t)+i\frac{B^2}{2}t}. \tag{11}$$

The equation for the envelope A then reads

$$\begin{aligned} A(t) = &\psi_R(-x_{cl}(t),t) + \frac{iB}{\sqrt{2\pi i}} \\ &\int_0^t dt' W(t,t')\exp\left\{\frac{i[x_{cl}(t)-x_{cl}(t')]^2}{2(t-t')}\right\}A(t'), \end{aligned} \tag{12}$$

where W represents a singular integration weight

$$W(t,t') = \frac{e^{+i\frac{B^2}{2}(t'-t)}}{\sqrt{t-t'}}, \tag{13}$$

and the right-hand side can be expressed using complementary error functions,

$$\psi_R(x,t) \equiv \frac{e^{+Bx}}{2}\mathrm{erfc}\left(\frac{iBt+x}{\sqrt{2it}}\right) + \frac{e^{-Bx}}{2}\mathrm{erfc}\left(\frac{iBt-x}{\sqrt{2it}}\right). \tag{14}$$

Equations (11)–(14) constitute the first step toward the evaluation of physical observables for an arbitrary time-dependent field. This integral equation has a singular kernel and is, in fact, closely related to the Abel integral equation [31]. A numerical solution of such equations requires care, but it can be done efficiently. We defer the implementation details to a later section in which we address numerical issues.

B. Elimination of classical current contributions

Since the transformation of (9) to an explicit form is rather lengthy, it is desirable to simplify this procedure. Importantly, the following reduction also eliminates, to a large degree, the mutual cancellation between different contributions in the final result. Let us consider the derivative terms in (9) and see that they receive contribution from two sources. The first is the argument of the free-particle propagator K_0 and the second is the phase ϕ of the Volkov propagator K_F. The latter results in multiplication by the classical momentum $p_{cl}(t)$. After factoring this out, we obtain

$$p_{cl}(t)\int dx\{\psi_F^*\psi_F + \psi_F^*\psi_S + \psi_S^*\psi_F + \psi_S^*\psi_S\}, \tag{15}$$

where the integral gives unity since it is the conserved norm of the full wave function. Thus, all contributions that originate from $\partial_x e^{i\phi(x,t,x',t')}$ will collectively yield $p_{cl}(t)$ and do not need to be evaluated explicitly. Moreover, they are linear in F and therefore not interesting for our purposes.

An alternative view of this reduction is to realize that norm conservation implies an identity that $A(t)$ must satisfy. Because ψ_F alone is a product of unitary evolution, its norm is equal to one at all times. Consequently, other contributions to the wave-function norm must mutually cancel,

$$\langle\psi_F|\psi_S\rangle + \langle\psi_S|\psi_F\rangle + \langle\psi_S|\psi_S\rangle = 0,$$

which can be evaluated explicitly to

$$\begin{aligned} &\mathrm{Re}\Bigg[-iB^{-1}\int_0^t dt_1 A^*(t_1) \\ &\times\left(e^{-Bx_{cl}(t_1)}\mathrm{erfc}\left\{\frac{(1+i)[Bt_1+ix_{cl}(t_1)]}{2\sqrt{t_1}}\right\}\right. \\ &\left.+e^{+Bx_{cl}(t_1)}\mathrm{erfc}\left\{\frac{(1+i)[Bt_1-ix_{cl}(t_1)]}{2\sqrt{t_1}}\right\}\right)\Bigg] \\ &= \frac{(-1)^{\frac{3}{4}}}{\sqrt{2\pi}}\int\int_0^t dt_1 dt_2 W(t_1,t_2)e^{\frac{i[x_{cl}(t_1)-x_{cl}(t_2)]^2}{2(t_1-t_2)}}A(t_2)A^*(t_1). \end{aligned} \tag{16}$$

This identity can be used to simplify expressions which are proportional to $p_{cl}(t)$. In what follows, we assume that either of the two reduction methods was used in the calculation, allowing us to omit all corresponding contributions. This amounts to ignoring $\partial_x\phi(x,t,x',t')$ whenever ∂_x acts on K_F.

Next, we split the calculation of the induced current into terms corresponding to Eq. (9). We are only interested in extracting the part of the current which is nonlinear in the driving field $F(t)$, and we will show how this can be done exactly.

C. Current contribution J_{FF}

The simplest term to evaluate is the current due to ψ_F,

$$J_{FF} = \mathrm{Im}\int dx \psi_F^* \nabla \psi_F.$$

The result can be deduced from the fact that ψ_F represents the movement of a free particle under an influence of an external force. Initially, this particle is in the ground state of the field-free Hamiltonian and has zero net momentum. Because the Volkov propagator action can be decomposed into free wave-packet spreading, followed by a classical shift in space by $x_{cl}(t)$ and and an increase in the particle's momentum by $p_{cl}(t)$, we can see that J_{FF} is equal to the following classical momentum:

$$J_{FF} = p_{cl}(t). \tag{17}$$

Naturally, the same result can be obtained by direct calculation, as shown in the Appendix. Because J_{FF} is linear in the driving field intensity $F(t)$, it does not contribute to the nonlinear current, which we aim to calculate.

D. Current contribution J_{SS}

Next, let us evaluate

$$J_{SS} = \mathrm{Im}\int dx \psi_S^* \nabla \psi_S, \tag{18}$$

and extract its nonlinear part $J_{SS}^{(nl)}$. After inserting the expression for the scattered wave-function component, and using the explicit form of the Volkov propagator, we can write

$$J_{SS} = \mathrm{Im}\left[B^3 \int_0^t \int_0^t dt_1 dt_2 A(t_2) A^*(t_1) I(t_1,t_2)\right], \tag{19}$$

where the quantity I represents the result of integration over the spatial variable x:

$$I(t_1,t_2) = \int dx \frac{[x - x_{cl}(t) + x_{cl}(t_2)]}{2\pi i (t-t_1)^{\frac{1}{2}}(t-t_2)^{\frac{3}{2}}} e^{i\frac{B^2}{2}(t_2-t_1)} \times e^{\frac{i[x-x_{cl}(t)+x_{cl}(t_2)]^2}{2(t-t_2)} - \frac{i[x-x_{cl}(t)+x_{cl}(t_1)]^2}{2(t-t_1)}}. \tag{20}$$

Note that the classical action phase from the propagator has been absorbed by the ansatz for $\psi(0,t)$. The integration order was exchanged between (18) and (19), which is justified when a small imaginary part is added to the time variable to make the integral over x convergent for fixed $t_{1,2}$. The integral is Gaussian, and can be evaluated directly as

$$I(t_1,t_2) = \frac{(-i)^{\frac{3}{2}}}{\sqrt{2\pi}} W(t_1,t_2) \frac{x_{cl}(t_1) - x_{cl}(t_2)}{t_1 - t_2} e^{\frac{i[x_{cl}(t_1)-x_{cl}(t_2)]^2}{2(t_1-t_2)}}. \tag{21}$$

It becomes evident that I is a function of $t_{1,2}$ but does not depend on t.

To further simplify the numerical evaluation, the double integral over the rectangle, $(0,t)\times(0,t)$, is split into integration over triangles, $\int_0^t dt_1 \int_0^t dt_2 = \int_0^t dt_1 \int_0^{t_1} dt_2 + \int_0^t dt_2 \int_0^{t_2} dt_1$. In the latter term, we rename $t_1 \leftrightarrow t_2$ and verify that the two integrals have complex-conjugate integrands.

At this point, we can eliminate the linear part of this current contribution. The classical position $x_{cl}(t)$ is linear in F, therefore, we must remove the zero-order part from the rest of the integrand in (19). The first field-dependent contribution from the exponential in $I(t_1,t_2)$ is of the second order, and $A(t)$ reduces to one for zero field. In order to remove the linear part of their product, we subtract unity from this expression, which appears when (21) is inserted in (19):

$$e^{\frac{i[x_{cl}(t_1)-x_{cl}(t_2)]^2}{2(t_1-t_2)}} A^*(t_1)A(t_2) \to e^{\frac{i[x_{cl}(t_1)-x_{cl}(t_2)]^2}{2(t_1-t_2)}} A^*(t_1)A(t_2) - 1.$$

The final result for the nonlinear current contribution from the scattering part of the wave function becomes

$$J_{SS}^{(nl)} = 2\mathrm{Im}\left\{\int_0^t dt_1 \int_0^{t_1} dt_2 \frac{(-i)^{\frac{3}{2}} B^3 W(t_1,t_2)}{\sqrt{2\pi}} \times \left[e^{\frac{i[x_{cl}(t_1)-x_{cl}(t_2)]^2}{2(t_1-t_2)}} A^*(t_1)A(t_2) - 1\right] \frac{x_{cl}(t_1) - x_{cl}(t_2)}{t_1 - t_2}\right\}. \tag{22}$$

Similar to the integral equation for $\psi(0,t)$, the integrand is singular when $t_2 \to t_1$. Fortunately, the singularity is not stronger, since the classical position difference vanishes and the corresponding fraction converges to the classical momentum. The discussion of the numerical aspects that are important in evaluating this expression is postponed to a dedicated section.

E. Current contribution J_{FS}

The mixed current contribution

$$J_{FS} = \mathrm{Im}\int dx (\psi_F^* \nabla \psi_S + \psi_S^* \nabla \psi_F) \tag{23}$$

is more difficult to calculate, but it simplifies to a rather compact final expression. Just as with J_{SS}, we will also systematically drop all contribution arising from $\partial_x \phi$, since we have established that their contribution is irrelevant for our purposes.

In this derivation, there are two spatial variables of integration. One is x and the other is the auxiliary variable originating in the initial state $\psi_G(z)$. Integration over z should be executed first; however, integrating first over x gives the same result with less work. When we insert explicit expressions for the wave-function components $\psi_{F,S}$, the integration order is changed such that $\int dx$ is done first. Again, the change of integration order is permissible if we assume a small imaginary part in the time variable, which makes the integrals convergent. At this stage, we obtain

$$J_{FS} = \mathrm{Im}\int dz \int_0^t dt_1 \sqrt{\frac{2}{\pi}} \frac{(-1)^{\frac{3}{4}} B^2}{t_1^{\frac{3}{2}}} \times e^{-i\frac{B^2}{2}t_1} e^{-B|z|} e^{\frac{i[z+x_{cl}(t)]^2}{2t_1}} A^*(t_1)[z + x_{cl}(t_1)], \tag{24}$$

where we have added two expressions coming from $\psi_F^* \nabla \psi_S$ and $\psi_S^* \nabla \psi_F$, respectively, with each contributing the same imaginary part.

Next, we perform integration over the variable z. This is done separately for $z < 0$ and $z > 0$, with each integration resulting in a number of terms containing error functions of complex arguments. Fortunately, considerable simplification occurs when the two parts are joined. Since multiple equivalent ways exist to represent the result, the most appropriate should be chosen with future calculations in mind. In particular, subtracting order-of-one quantities at large negative and positive times should be avoided. A compact form suitable for numerical evaluation can be given using complementary error functions,

$$J_{FS} = \mathrm{Im}\Bigg[iB^3 \int_0^t dt_1 A^*(t_1) \Bigg(e^{+Bx_{cl}(t_1)} \times \mathrm{erfc}\left\{ \frac{(1+i)[Bt_1 - ix_{cl}(t_1)]}{2\sqrt{t_1}} \right\} - e^{-Bx_{cl}(t_1)} \times \mathrm{erfc}\left\{ \frac{(1+i)[Bt_1 + ix_{cl}(t_1)]}{2\sqrt{t_1}} \right\} \Bigg) \Bigg]. \tag{25}$$

This is not our final result, since J_{FS} still contains contributions linear in $F(t)$. Note that the expression in square brackets is an odd function of $x_{cl}(t)$ and, by the same token, an odd function of F. Thus, the first-order term of the Taylor expansion in x_{cl} will be subtracted in order to cancel the unwanted linear response,

$$J_{FS}^{(nl)} = J_{FS} - \mathrm{Im}\left(2B^3 \int_0^t dt_1 x_{cl}(t_1) \times \left\{ iB\ \mathrm{erfc}\left[\frac{(1+i)B\sqrt{t_1}}{2} \right] - \frac{1+i}{\sqrt{\pi t_1}} e^{-i\frac{B^2}{2}t_1} \right\} \right), \tag{26}$$

where we have again used that as $F \to 0$, $A(t) \to 1$. Expressions (25) and (26) together with (22) constitute our final result. They allow us to calculate the exact nonlinear current induced by an arbitrary time-dependent field $F(t)$. An accurate evaluation of these formulas requires care, therefore, we will address ways to implement them in the form of efficient, robust algorithms in the next section.

IV. IMPLEMENTATION AND VERIFICATION

In summary, the procedure used to calculate the current induced by an optical-frequency pulse characterized by the field strength $F(t)$ consists of

(1) calculating the quantities related to the classical electron trajectory, i.e., $p_{cl}(t)$, $x_{cl}(t)$, and $S_{cl}(t)$,

(2) solving the integral equation for $A(t)$ as specified in Eqs. (11)–(14), and

(3) evaluating the nonlinear current contributions from Eqs. (22), (25), and (26).

If the time-dependent quantities are represented on a grid with N_t sampling points, the computational complexity of this procedure scales as N_t^2. Therefore, it is important to design an algorithm which can be accurate even with a long temporal step.

Integrals with the singular integration weight (13) must be calculated both in the integral equation for $A(t)$ and in J_{SS}. To achieve an acceptable accuracy for time steps as long as one-tenth of the atomic unit of time, the singularity must be treated analytically. To do this, we calculate an integral of the form

$$\int_0^t W(t,\tau) f(\tau),$$

with a representation of f sampled on a discrete set $\{\tau_i\}$. This allows the approximation

$$\int_{\tau_i}^{\tau_{i+1}} W(t,\tau) f(\tau) = \int_{\tau_i}^{\tau_{i+1}} W(t,\tau) P(\tau),$$

where $P(\tau)$ is an interpolating polynomial of $\{f(\tau_i)\}$ spanning a vicinity of the interval (τ_i, τ_{i+1}). We have tested linear and second-order methods, and have concluded that the first-order method is accurate enough to not warrant restricting the time step. With the locally linear approximation to f, the integral over a subinterval is then given by pre-calculated weights,

$$\int_{\tau_i}^{\tau_{i+1}} W(t,\tau) f(\tau) = w(t,i) f(\tau_i) + w(t,i+1) f(\tau_{i+1}).$$

Note that for a regular temporal grid, only a single weight vector $w(i-j)$ needs to be stored. The same is true for an order-n method, which requires n integration weight vectors $w^{(n)}(k)$. Explicit expressions for these integration weights depend on the ground-state energy $B^2/2$, and can be readily calculated in terms of error functions with complex arguments. The resulting integration algorithm is fast, as it only requires several multiplications per grid point.

When solving the integral equation for $A(t)$, we evolve the solution along the temporal axis as the formula suggests. At each point t_c, integration over its past, $\int_0^{t_c - \Delta t}$, is performed using the above scheme. This is why the method scales as N_t^2. The same scheme is also applied to the last subinterval, $\int_{t_c-\Delta t}^{t_c}$, with the current endpoint carrying the unknown $A(t_c)$. The endpoint value then appears on both sides and can be expressed.

The singular integration scheme is also applied to the inner integral in $J_{SS}^{(nl)}$. For the outer integral, we have used integration rules of various orders, and found that a simple first-order scheme is satisfactory.

The numerical evaluation of $J_{FS}^{(nl)}$ requires the calculation of complex complementary error functions. Because they are dependent on the classical position x_{cl}, these quantities cannot be precalculated. Consequently, an implementation for erf(z) that works in the entire complex plane is required. We have chosen the algorithm implemented in the open-source IT++ library.

To verify that our implementation of the nonlinear current produces correct results, we performed comparisons with solutions obtained from direct numerical simulations of the time-dependent Schrödinger equation (1). The δ-function potential was implemented as a condition specifying the value at the cusp of the derivative located at the origin as stated by (2). The time-stepping scheme was taken from [32], and reflecting boundary conditions were used at the edges of the computational domain.

We choose to show an illustration for the time-dependent dipole moment instead of the current because dipole-moment plots are more intuitive, as their low-frequency components

are more prominent and resemble the temporal shape of the driving pulse.

In order to facilitate a comparison with the nonlinear component of the induced dipole moment, the latter was extracted from two simulations that used the same temporal shape of the driving pulse:

$$P^{(nl)} = \lim_{S\to\infty} [P(\{F(t)\}) - SP(\{F(t)/S\})].$$

Here, the second simulation occurs at a very low intensity and represents the linear (in F) contribution to the total polarization P. The scaling factor S reduces the driving field amplitude to where observed nonlinear effects become negligible. Subtracting the linear part leaves us with the nonlinear response, which can be compared to our calculations using analytic formulas.

A rather fine grid resolution and short integration step was required for the time-domain Schrödinger equation (TDSE) simulation, which generated the comparison data sets shown here. We used a numerical grid with the spacing of 0.025 (in atomic units) and 50 000 points, and the time step was only 0.00025 (in atomic units).

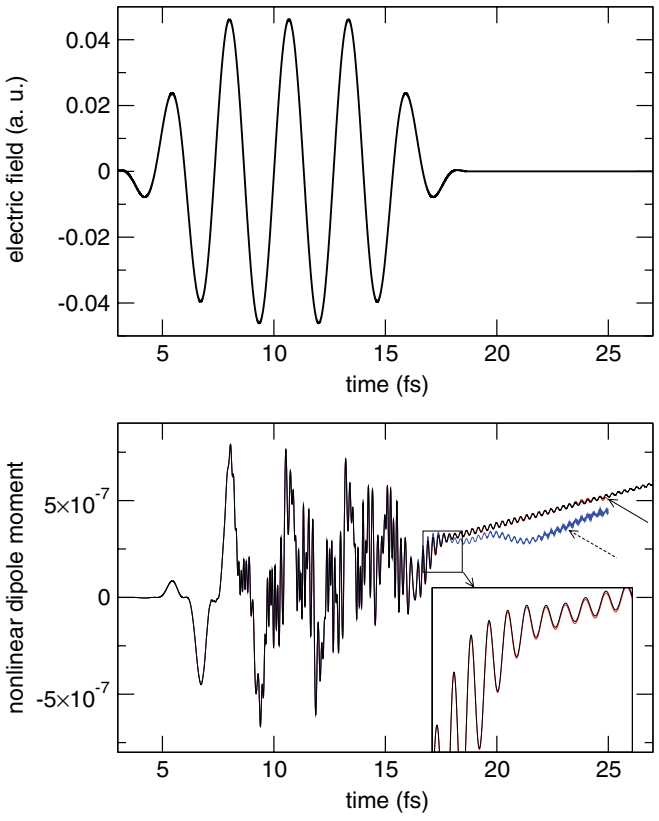

FIG. 1. (Color online) Verification of the implementation of analytic formulas for nonlinear response. The lower panel shows a comparison with TDSE simulations of nonlinear dipole-moment response to the driving pulse shown in the upper panel. The black curve is based on the formulas we have derived. The blue curve (dashed arrow) represents the TDSE simulation on a smaller grid. The barely visible red curve (full arrow indicates its end) is the TDSE result for a larger grid. This shows that deviations between analytic results and direct numerics occur solely due to finite-size effects in the latter. Note that these calculations do not contain the linear part of the response.

Figure 1 shows our analytic calculation compared to the TDSE simulations performed with two different domain sizes. Perfect agreement is achieved for a sufficiently large TDSE domain, verifying that our implementation of the analytic expressions for the nonlinear current is indeed correct. Deviations only occur when the TDSE numerical grid is too small to accommodate the spreading wave function in the later stages of evolution. Analytic solutions do not suffer from such finite-size artifacts thanks to the fact that the spatial variable has been integrated out.

Having verified the correctness of the implementation, the question of stability of our method must be addressed. Because the algorithm mimics the evolution of the current components along the time axis, instability could prevent its practical application. While we have no formal proof that the method is stable, we have observed no indications of the opposite, even when using extremely long temporal grids containing a few-hundred-thousand points. We take this as a strong indication that the numerical implementation as described in this section is indeed stable.

To complete this section, we want to illustrate the utility of our results for the field of high-harmonic generation (HHG) driven by ultraintense, femtosecond-duration optical pulses. Figure 2 shows an example of the spectrum of high harmonics in the nonlinear current driven by an infrared optical pulse. Such nonlinear response can be integrated into a carrier-resolving pulse propagation solver, such as the unidirectional pulse propagation equation (UPPE) [33], to model the generation, buildup, and subsequent propagation of harmonic radiation.

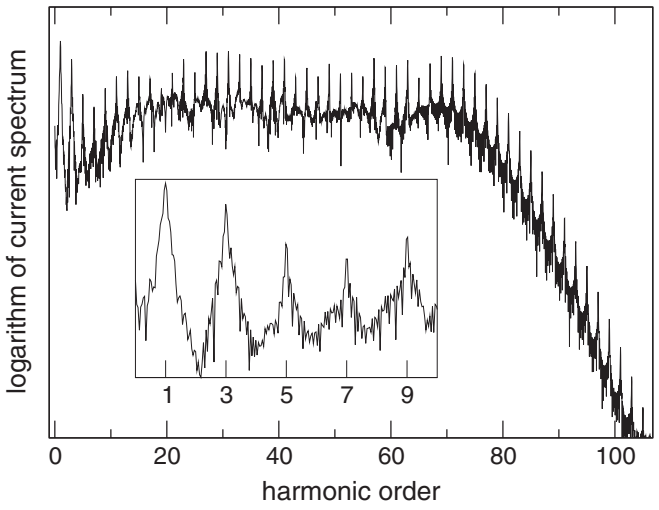

FIG. 2. High-harmonic spectrum of the nonlinear current induced by a $\lambda = 1.3\ \mu$m pulse. The intensity of the driving field was 10^{18} Wm^{-2}, constant during 13 optical cycles, and with leading and trailing ramps of four-cycle duration. The inset shows the detail of the spectrum for low harmonics. Unlike in the strong-field approximation, low-frequency current and dipole-moment components are exact, and can be included in the Maxwell equation solver as a source which affects the propagation of the pump pulse.

Importantly, the present quantum model takes on several model "functions" that are normally implemented as independent components in such simulations. Namely, it provides a mechanism for ionization, describes the current due to free electrons, and also contributes the Kerr-type nonlinearity originating in bound-to-continuum transitions. Moreover, it generates the lower harmonics, including fundamental, and thus significantly contributes to reshaping of the pump pulse. Because ours is an exact solution, there is no question about all of these effects being mutually consistent, which can hardly be said about the present models used in the simulations of optical filamentation and harmonic generation.

We want to emphasize that while the model requires significant computation, the numerical effort to evaluate the current formulas is acceptable, even for fully spatially resolved Maxwell-Schrödinger systems. To give at least a rough idea, a simple filament simulation may currently take 50 hours. This may be 10 times longer than one using the standard model, but qualitative studies are indeed feasible. However, the description of how this quantum calculation for the atomic nonlinear response can be integrated with a pulse propagation simulator is far beyond the scope of this paper, and will be discussed in a dedicated work.

V. CONCLUSION

We have extended the range of exact results for the quantum model of a one-dimensional particle with a short-range contact potential, moving under the influence of an arbitrary time-dependent external field. Specifically, we have derived expressions for both the current and dipole moment, and extracted their components that are nonlinear with respect to the driving field. With applications in mind, we also described an algorithm for numerical evaluation, and demonstrated its robust implementation. Typically, a temporal grid will contain up to 10 000 points, and a single solution will take a few seconds. This is indeed a significant effort, but an acceptable price for an exact solution of a quantum system.

Our results will be useful in the general area of high-intensity light-matter interactions, where they can be used as a testbed system for theories and simulation methods, which describe strongly nonlinear evolution on an extremely short time scale. In particular, in the field of optical filamentation, they can serve as a tool to study possible improvements to current models, especially the parts concerning ionization and free electrons. Because the present model, having only one bound state, does not contribute Kerr nonlinearity originating in the bound-to-bound transitions, one can combine the standard instantaneous Kerr effect, frequency-dependent linear susceptibility, and this one-dimensional quantum system into a self-consistent, qualitative model for femtosecond filamentation. For the area of high-harmonic generation, the derived current and dipole formulas represent an exactly solvable alternative to the widely used strong-field approximation. Moreover, they unify treatment of the pump and harmonic radiation.

Obviously, one limitation of the presented results lies in the one-dimensional nature of the underlying model. However, many works have been published on higher-dimensional exactly solvable models related to the system studied here. In particular, it will be interesting to investigate the possibility of generalizing our results for models with the so-called δ-shell potentials (see, e.g., [34]) in three dimensions.

ACKNOWLEDGMENTS

The authors acknowledge support by the US Air Force Office for Scientific Research, through the multiuniversity research initiative, "Mathematical Modeling and Experimental Validation of Ultrashort Nonlinear Light-Matter Coupling associated with Filamentation in Transparent Media," Grant No. FA9550-10-1-0561.

APPENDIX

1. Explicit calculation of J_{FF}

To evaluate current J_{FF}, we first calculate the spatial integral within $\psi_F(x,t)$ in order to appreciate its symmetry with respect to the classical electron position x_{cl}. The direct integration of a Gaussian integral yields

$$\psi_F(x,t) = \frac{1}{2}\sqrt{B}e^{ixp_{cl}(t)-iS_{cl}(t)}e^{\frac{1}{2}iB^2t} \times \left\{e^{B[+x-x_{cl}(t)]}\mathrm{erfc}\left[\frac{+x-x_{cl}(t)+iBt}{\sqrt{2it}}\right] + e^{B[-x+x_{cl}(t)]}\mathrm{erfc}\left[\frac{-x+x_{cl}(t)+iBt}{\sqrt{2it}}\right]\right\} \quad \text{(A1)}$$

(see Elberfeld *et al.* [14]). With the help of ψ_R (14), we separate the phase term,

$$\psi_F(x,t) = \sqrt{B}e^{ixp_{cl}(t)-iS_{cl}(t)}e^{\frac{1}{2}iB^2t}\psi_R[x-x_{cl}(t)]. \quad \text{(A2)}$$

The only property we need to use is that ψ_R is a symmetric function. We insert $\psi_F(x,t)$ and its conjugate into J_{FF}, and substitute $y = x - x_{cl}(t)$, to obtain

$$J_{FF} = \int_{-\infty}^{+\infty} dy\, \psi_R^*(y,t)\frac{d}{dy}\psi_R(y,t) + p_{cl}(t)\int_{-\infty}^{+\infty} dy\, \psi_F^*(y,t)\psi_F(y,t). \quad \text{(A3)}$$

The first integrand is an odd function, so the first term vanishes upon integration. The second integral multiplied by $p_{cl}(t)$ is equal to one, since $\psi_F(y,t)$ is normalized. The result is as in (17): $J_{FF} = p_{cl(t)}$.

2. Summary of results for the time-dependent dipole moment

Evolution of the dipole moment induced by an external field can be calculated in the same manner as the current. The calculation is somewhat more involved, and the structure of the final result is also less suitable for numerical evaluation. Since the current and dipole observables can be converted from one to the other by integration with respect to time, in practical applications, users will likely choose the former. However, we chose to complete the picture with explicit expressions of exact time-dependent dipole-moment formulas.

The full dipole moment is decomposed into components analogous to those we used for the current,

$$P = P_{FF} + P_{FS} + P_{SS}. \quad \text{(A4)}$$

In order to make the relationship between dipole and current derivations more apparent, we will not eliminate the linear

part. The first contribution is obtained utilizing a symmetry argument,

$$P_{FF} = x_{cl}(t), \tag{A5}$$

and the P_{SS} component can be written in the following form, which makes it easy to verify that its time derivative corresponds to J_{SS} as expected:

$$P_{SS} = 2\mathrm{Re}\left\{ \int_0^t dt_1 \int_0^{t_1} dt_2 \frac{(-1)^{\frac{3}{4}} B^3 W(t_1,t_2)}{\sqrt{2\pi}} e^{\frac{i[x_{cl}(t_1)-x_{cl}(t_2)]^2}{2(t_1-t_2)}} A^*(t_1)A(t_2) \frac{x_{cl}(t)(t_1-t_2)+x_{cl}(t_1)(t_2-t)+x_{cl}(t_2)(t-t_1)}{t_1-t_2} \right\}. \tag{A6}$$

The derivative with respect to the upper integration bound vanishes due to the symmetry of the integrand. If one takes the derivative of the integrand with respect to t, it gives the expression we have found for J_{SS}. Similarly, P_{FS} can be put in a form which makes it evident that $\partial_t P_{FS} = J_{FS}$. This term evaluates to

$$\begin{aligned} P_{FS} = \mathrm{Re}\Bigg[iB^2 \int_0^t dt_1 A^*(t_1) \Bigg(& e^{-Bx_{cl}(t_1)} \mathrm{erfc}\left\{ \frac{(1+i)[Bt_1 + ix_{cl}(t_1)]}{2\sqrt{t_1}} \right\} [x_{cl}(t1) - x_{cl}(t) + iB(t-t_1)] \\ & + e^{+Bx_{cl}(t_1)} \mathrm{erfc}\left\{ \frac{(1+i)[Bt_1 - ix_{cl}(t_1)]}{2\sqrt{t_1}} \right\} [x_{cl}(t1) - x_{cl}(t) - iB(t-t_1)] \Bigg) \Bigg]. \end{aligned} \tag{A7}$$

Note that both P_{SS} and P_{FS} contain terms proportional to $x_{cl}(t)$. If these are collected, the identity (16) is obtained, which means that their sum is zero and they can be ignored.

Even with this cancellation, the dipole representation is more difficult to evaluate when compared to the current. This is mainly due to the fact that time t appears inside both integrands. If coded as written, this method's complexity would scale as N_t^3. This unfavorable behavior can be reduced to N_t^2 with clever programming, but the resulting algorithm is still more complex than that of the current. This is why in applications it will be more effective to calculate time-dependent current. If the dipole moment is required, it can be obtained by integrating along the time axis. To convert the dipole moment from atomic units to medium polarization, we simply multiply by ea_0N, the product of electron charge, atomic unit of length, and the number density of atoms per unit of volume. Regardless of the calculation method, either the current or dipole moment can be used in a pulse propagation simulator, since they produce equivalent driving terms in the optical evolution equations.

[1] A. Couairon and A. Mysyrowicz, Phys. Rep. **441**, 47 (2007).
[2] L. Bergé, S. Skupin, R. Nuter, J. Kasparian, and J. Wolf, Rep. Prog. Phys. **70**, 1633 (2008).
[3] S. Suntsov, D. Abdollahpour, D. G. Papazoglou, and S. Tzortzakis, Opt. Express **17**, 3190 (2009).
[4] Yi Liu, M. Durand, A. Houard, B. Forestier, A. Couairon, and A. Mysyrowicz, Opt. Commun. **284**, 4706 (2011).
[5] V. Loriot, E. Hertz, and O. Faucher, Opt. Express **17**, 13429 (2009).
[6] M. A. Naimark, *Linear Differential Operators* (Dover, New York, 2012).
[7] P. Šeba, Czech. J. Phys. **36**, 455 (1986).
[8] M. G. Krein, Dokl. Akad. Nauk SSSR **52**, 657 (1946) [Sov. Phys. Dokl.].
[9] R. M. Cavalcanti, P. Giacconi, and R. Soldati, J. Phys. A **36**, 12065 (2003).
[10] H. L. Cycon, R. Froese, W. Kirsch, and B. Simon, *Schrödinger Operators* (Springer-Verlag, Berlin, 1987).
[11] S. Albeverio and P. Kurasov, *Singular Perturbations of Differential Operators* (Cambridge University Press, Cambridge, 2000).
[12] S. Geltman, J. Phys. B **11**, 3323 (1978).
[13] G. P. Arrighini and M. Gavarini, Lett. Nuovo Cimento **33**, 353 (1982).
[14] W. Elberfeld and M. Kleber, Z. Phys. B **73**, 23 (1988).
[15] G. V. Dunne and C. S. Gauthier, Phys. Rev. A **69**, 053409 (2004).
[16] G. Álvarez and B. Sundaram, J. Phys. A **37**, 9735 (2004).
[17] H. Uncu, H. Erkol, E. Demiralp, and H. Beker, Centr. Eur. J. Phys. **3**, 303 (2005).
[18] V. M. Villalba and L. A. González-Díaz, Eur. Phys. J. C **61**, 519 (2009).
[19] A. Teleki, E. M. Wright, and M. Kolesik, Phys. Rev. A **82**, 065801 (2010).
[20] Q. Su, B. P. Irving, C. W. Johnson, and J. H. Eberly, J. Phys. B **29**, 5755 (1996).
[21] S. Geltman, J. Phys. B **27**, 1497 (1994).
[22] T. Grozdanov, P. Krstic, and M. Mittleman, Phys. Lett. A **149**, 144 (1990).
[23] J. Mostowski and J. H. Eberly, J. Opt. Soc. Am. B **8**, 1212 (1991).
[24] A. Sanpera, Q. Su, and L. Roso-Franco, Phys. Rev. A **47**, 2312 (1993).
[25] T. Mercouris and C. A. Nicolaides, J. Phys. B **33**, 2095 (2000).
[26] J. Matulewski, A. Raczyński, and J. Zaremba, Phys. Rev. A **61**, 043402 (2000).
[27] X. Zhou, B. Li, and C. D. Lin, Phys. Rev. A **64**, 043403 (2001).
[28] Z. X. Zhao, B. D. Esry, and C. D. Lin, Phys. Rev. A **65**, 023402 (2002).
[29] V. D. Rodríguez and R. O. Barrachina, Eur. Phys. J. D **64**, 593 (2011).

[30] T. Dziubak and J. Matulewski, Eur. Phys. J. D **59**, 321 (2010).
[31] K. E. Atkinson, SIAM Numer. Anal. **11**, 97 (1974).
[32] P. B. Visscher, Comp. Phys. **5**, 596 (1991).
[33] M. Kolesik and J. V. Moloney, Phys. Rev. E **70**, 036604 (2004).
[34] J. P. Antoine, F. Gesztesy, and J. Shabani, J. Phys. A **20**, 3687 (1987).